Neurochemistry International 194 (2026) 106123

Contents lists available at ScienceDirect

Neurochemistry International

journal homepage: www.elsevier.com/locate/neuint

Calcineurin inhibition mitigates activation of enteric glia *in vitro* and affects their crosstalk with macrophages

Aurora Patti [a], Cristiana Lucia Rita Lipari [a], Armando Genazzani [b], Maria Angela Sortino [a,*], Sara Merlo [c,**]

[a] Department of Biomedical and Biotechnological Sciences, University of Catania, Italy
[b] Department of Scienza e Tecnologia del Farmaco, University of Turin, Italy
[c] Department of Drug and Health Sciences, University of Catania, Italy

ARTICLE INFO

Keywords:
Inflammatory bowel diseases (IBD)
Enteric glial cells
Macrophages
Calcineurin
Cyclosporin A

ABSTRACT

Multiple factors contribute to the physiopathology of inflammatory bowel diseases (IBD) and the enteric nervous system is emerging as a key player in this context. In particular, enteric glial cells (EGCs) share very similar properties with central astrocytes, play a homeostatic function under basal conditions, but can be activated by inflammatory stimuli further contributing to mucosal damage. Calcineurin (CN) is an important mediator of astrocyte inflammation and has been described also in EGCs. The aim of this study was to establish an *in vitro* model of EGCs challenged with an inflammatory insult to better delineate the role of CN in their inflammatory reaction and interaction with immune cells. EGCs stimulated with LPS + ATP (5 μg/mL-2 mM) for 24 h showed typical inflammatory features with increased expression of the astrocyte marker GFAP, the inflammasome component NLRP3 and the alarmin HMGB1. Inhibition of CN by cyclosporin A (CsA, 1 μM) counteracted these effects and increased the expression of nuclear HMGB1. Nuclear translocation of NF-κB p65 induced by LPS + ATP was also blunted by CsA pre-treatment. The migration of RAW 264.7 macrophages co-cultured with LPS + ATP-stimulated EGCs was enhanced, an effect prevented by CsA. This was accompanied by activation of macrophages to a pro-inflammatory phenotype, as shown by increased COX-2, IL-1β and TNF-α gene expression. Inhibition of CN in EGCs reduced this response while increasing the phagocytic capacity of macrophages. Altogether the results here reported identify a central role for CN in the inflammatory response of EGCs and their crosstalk with cells of the immune system, supporting potential new sites of intervention for drugs targeting CN.

1. Introduction

Inflammatory bowel diseases (IBD), including Crohn's disease (CD) and ulcerative colitis (UC), are chronic immune-mediated conditions for which treatment options remain limited, partly due to a multifactorial pathogenic mechanism that is not yet fully understood. Current data suggest that IBD may result from a complex interaction between genetic predispositions, environmental factors and abnormal immune responses (Zeng et al., 2019). In addition, recent evidence implicates alterations in the enteric nervous system (ENS) in IBD etiology (Suman, 2024). The ENS is a peripheral neural network that integrates and controls essential gastrointestinal functions, via 'brain-like' circuitry composed of neurons and glia. Enteric glial cells (EGCs) can be considered analogous to astrocytes in the central nervous system (CNS). They share morphological and functional similarities, as well as many common markers such as glial fibrillary acidic protein (GFAP) and S100 calcium-binding protein B (S100B) (Santhosh et al., 2024; Seguella and Gulbransen, 2021). Under physiological conditions, enteric glia is involved in maintaining homeostasis and supporting neurons, as well as contributing to the preservation of the intestinal epithelial barrier integrity. EGCs also give life to a reciprocal cross-talk with immune cells, differently affecting local responses in the course of IBD (Liu and Yang, 2022; Schneider et al., 2025). In particular, in the presence of inflammatory stimuli, enteric glia can convert to a reactive phenotype capable of sustaining the chronicization of a local pro-inflammatory state. This is characterized by an increased expression of GFAP and the release of S100B, which in turn promotes the production of NO and of pro-inflammatory cytokines via the nuclear factor κ-light-chain-enhancer of activated B cells (NF-κB)

* Corresponding author.
** Corresponding author.
E-mail addresses: msortino@unict.it (M.A. Sortino), sara.merlo@unict.it (S. Merlo).

https://doi.org/10.1016/j.neuint.2026.106123
Received 23 December 2025; Received in revised form 28 January 2026; Accepted 1 February 2026
Available online 3 February 2026

p65 activation (Capoccia et al., 2015; Cirillo et al., 2009). These events ultimately compromise the integrity of the mucosa (Cirillo et al., 2011; Liu and Yang, 2022; Ochoa-Cortes et al., 2016; Suman, 2024). An important mediator of glial inflammation, found both in CNS astrocytes and EGCs, is calcineurin (CN), a ubiquitously expressed calcium/calmodulin (CaM)-dependent serine/threonine phosphatase. CN is a key effector of Ca^{2+} signaling in eukaryotes, from fungi to mammals. In the latter, CN is expressed in all tissues but with higher levels in the immune, nervous and cardiovascular systems. Accordingly, its overexpression or dysfunction are associated with the development of several diseases, including immune system disorders, cardiomyopathies, renal and neurodegenerative diseases (Chen et al., 2022; Molkentin, 2004). CN is sensitive to rises in intracellular calcium levels and is activated by the dual binding to Ca^{2+} and to Ca^{2+}/CaM. The canonical pathways activated by CN involve dephosphorylation and nuclear translocation of the nuclear factor of activated T-cells (NFAT) and NF-κB p65 transcription factors. In T cells, this promotes the expression of interleukin (IL)-2 and several other pro-inflammatory cytokines (Furman and Norris, 2014; Ulengin-Talkish and Cyert, 2023). In the CNS, CN similarly mediates context-dependent pro-inflammatory activation in glial cells, but it also plays a homeostatic role, regulating glial and neuronal functions such as neuronal excitability and memory formation, glutamate uptake and gap junction conductance (Furman and Norris, 2014; Kipanyula et al., 2016; Lim et al., 2023; Tapella et al., 2020). Substantial changes in CN expression in glial cells have been associated with aging and neurodegenerative conditions, including Alzheimer's disease, as well as with other brain disorders (Furman and Norris, 2014; Kipanyula et al., 2016). In enteric glial cells, the role of CN has been mainly studied in knock-out mice. In these animals, the chronic lack of function throughout development seemed to impair gut formation and physiological activities such as motility and absorption, contributing to an inflammatory state (Fujita et al., 2018; Okura et al., 2019). However, to our knowledge, no study has so far investigated the role of CN activation in enteric glia during inflammatory conditions and the effects of acute CN inhibition, which offer insight beyond the developmental or genetic models of CN ablation. These conditions occur during IBD, where CN-directed immunosuppressant drugs have proven beneficial and are currently used as off-label options.

On these bases, we here aimed to fill this gap of knowledge by investigating whether CN pharmacological blockade could reduce enteroglial pro-inflammatory activation and indirectly affect the local immune response mediated by macrophages. We set up an *in vitro* model allowing us to more easily dissect the effects of CN blockade in inflamed enteric glia using immunosuppressant drug cyclosporin A (CsA). The results obtained contribute to shed new light on additional cellular targets and protective mechanisms of immunosuppressants in IBD.

2. Materials and methods

2.1. Drugs and reagents

Cyclosporin A (CsA; Cat. No. 30024; Merck, Darmstadt, Germany) was dissolved in dimethylsulfoxide (DMSO; Merck) as a 10 mM stock, and always added 15 min before other drugs. Lipopolysaccharide (LPS; Cat. No. L439, Merck) was dissolved in phosphate-buffered saline (PBS) as a 1 mg/mL stock and ATP (Cat. No. 1191; Merck) was dissolved in water as a 100 mM stock. Both were subsequently diluted in culture medium for experiments.

2.2. Cell cultures

EGC/PK060399egfr enteroglial cells (EGCs; Cat. No. CRL-2690, ATCC Manassas, VA, USA) and RAW 264.7 macrophages (Cat. No. TIB71, ATCC) were grown and maintained in Dulbecco's modified Eagle's medium (DMEM) supplemented with 10% of fetal bovine serum (FBS), sodium pyruvate (1 mM) and penicillin (100 U/mL)/streptomycin (100 μg/mL) at 37 °C and in a 5% CO_2 atmosphere. Media and supplements were all from Thermofisher Scientific (Waltham, MA, USA). EGCs were always plated at least 24 h before treatment and serum-deprived at the time of treatment. For conditioned medium (CM) experiments, EGCs were pre-exposed to drugs for 5 h, washed and incubated in fresh medium devoid of drugs for further 18 h. At the end of incubation, CM was collected and centrifuged at 1600 rpm for 5 min to remove debris and immediately transferred to RAW 264.7 macrophages. For transwell migration experiments, EGCs alone were pre-exposed to drugs for 5 h, washed and subjected to medium change prior to co-incubation for further 24 h, without drugs, with the macrophage-containing transwell insert. A detailed description of all treatment protocols is reported in the Results section, Fig. 1. All plastics, unless otherwise specified, were from Falcon Corning (Brookings, SD, USA).

2.3. 3-(4, 5-dimethylthiazolyl-2)-2, 5-diphenyltetrazolium bromide (MTT) assay

EGCs were plated at a density of 20k cells/well in a 96-well microplate and treated on the following day with LPS (5 μg/mL) for 23 h and ATP (2 mM) added during the last hour of incubation. MTT (Merck) was added to the medium at a final concentration of 0.5 mg/mL and cells were further incubated for 2 h at 37 °C. The medium was removed and formazan solubilization was carried out by incubation with DMSO for 10 min at 37 °C. The absorbance of solubilized formazan crystals was measured at 545 nm with VarioskanTM Flash Multimodal Reader (Thermofisher).

2.4. Immunocytochemistry

EGCs were seeded at a density of 15k cells/well in an 8-chamber permanox μslide (Thermo Scientific™ Nunc™ Lab-Tek™). After 24 h of treatment, cells were processed for immunostaining using the Inside Stain Kit (Cat. No. 130-090-477; Miltenyi Biotec, Bologna, Italy). Cells were first fixed using the InsideFix Solution, then incubated overnight at 4 °C with rabbit anti-HMGB1 (1:600; Cat. No. ab18256; Abcam) rabbit anti- NF-κB p65 (1:600; Cat. No.#8242; Cell Signaling, Danvers, MA, USA) or mouse anti TNFα-stimulated gene-6 (TSG-6) (1:50; cat # 377277; Santa Cruz Biotech. Santa Cruz, CA) diluted in the InsidePerm solution. After washing, cells were incubated with Alexa Fluor (AF)-546-conjugated anti-rabbit secondary antibody (1:300; Cat. No. A10040; Thermofisher) or AF-488 Plus-conjugated anti-mouse (1:300, Cat. No. A32790; Thermofisher), diluted in InsidePerm solution, for 45 min at RT. Slides were mounted with 4′,6-diamidino-2-phenylindole (DAPI)-containing Fluoroshield (Merck) and digital images were captured with a Zeiss Observer.Z1 microscope (Zeiss, Oberkochen, Germany) at 20X magnification. The number of immunopositive cells with nuclear HMGB1 and NF-κB p65 was determined by manual cell count in at least five randomly selected fields/well and reported as a percentage of total cells per field. All counts were carried out with the aid of the Image J software, developed by the National Institutes of Health (NIH) and in the public domain (Schneider et al., 2012).

2.5. Western blot

EGCs were seeded in 35 mm-dishes at a density of 600k cells/each and treated the next day for 24 h. At the end of treatment, cells were collected and lysed in radioimmunoprecipitation assay buffer (RIPA) (Thermofisher) supplemented with anti-protease and anti-phosphatase cocktails (Merck). Samples were sonicated, centrifuged at high speed for 10 min at 4 °C, and protein concentration was determined by micro-Bradford reagent (Thermofisher), according to the manufacturer's instructions. Absorbance was measured with a Varioskan™ Flash Multimode Reader. Sodium dodecyl sulphate-poly-acrylamide gel electrophoresis (SDS-PAGE) was performed by loading equal amounts of protein extracts/lane on pre-cast 4-20% gradient gels (Bio-Rad,

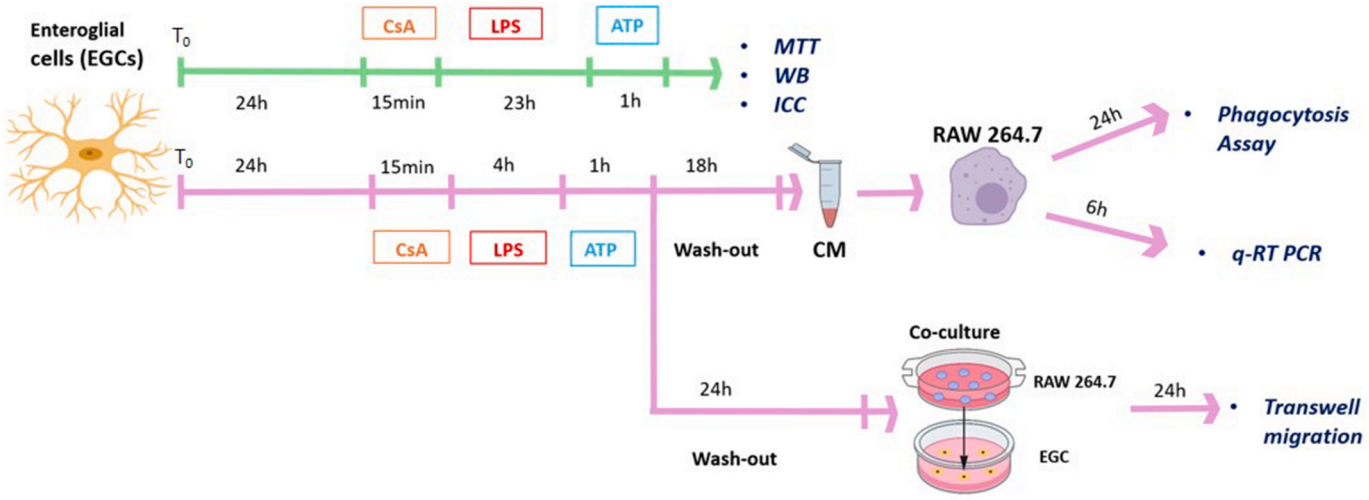

Fig. 1. Experimental model. Enteric glial cells (EGCs) and macrophages (RAW 264.7) were treated and processed as indicated. T_0 indicates time zero, corresponding to seeding of EGCs. WB: Western blot; ICC: immunocytochemistry, qRT-PCR: quantitative real-time PCR.

Hercules, CA, USA) and followed by transfer to nitrocellulose membranes (Hybond ECL, Amersham Biosciences Europe GmbH, Milan, Italy) using a Transblot semidry transfer cell (Bio-Rad, Hercules, CA, USA). Membranes were blocked with a Blocker FL Fluorescent Blocking buffer (Thermofisher) and incubated with primary antibodies overnight at 4 °C. Primary antibodies used were: rabbit anti-NLRP3 (1:500; Cat. No. #15101; Cell Signaling), mouse anti-GFAP (1:500; Cat.No. #3670; Cell Signaling), rabbit anti-HMGB1 (1:1000; Cat.No. ab18256; Abcam) and rabbit anti-β-actin (1:5000; Cat.No. A2066; Merck). Membranes were then washed and exposed to appropriate secondary antibodies for 45 min at room temperature (RT) as follows: AF-647-conjugated anti-rabbit (1:2000; Cat. No. A31573; Thermofisher) and AF-488 Plus-conjugated anti-mouse (1:5000; Cat. No. A32790; Thermofisher). The detection of specific bands was carried out using the iBright FL1500 Imaging System (Thermofisher). Band intensity was analyzed using the ImageJ software. All blots were cropped to display the specific bands of interest.

2.6. Quantitative real-time polymerase chain reaction (qRT-PCR)

RAW 264.7 macrophages were seeded in 35 mm-dishes at a density of 1.2 million cells/each. After 24 h, cells were exposed for 6 h to the CM obtained from EGCs as described above. Total RNA was extracted with the RNeasy Plus Mini Kit (Cat. No. 74134; Qiagen, Milan, Italy). RNA concentration was determined using Nanodrop ND-1000 (Thermofisher), and 1 μg of RNA was reverse transcribed with the QuantiTect Reverse Transcription Kit (Cat. No. 205311; Qiagen), according to the manufacturer's instructions. qRT-PCR was performed on Rotor-Gene Q (Qiagen) using the QuantiNova SYBR Green Real-Time PCR Kit (Cat. No. 20805; Qiagen) and the primers listed in Table 1. Samples were diluted at 1:60 for amplification. Melting curve analysis confirmed the specificity of the amplified products. Data analysis was carried out by the ΔΔCt method, using RPS18 for normalization, and expressed as fold change vs. the designated control.

Table 1
Primers used for qRT-PCR (all from Qiagen).

Gene	Primer	Cat. No.
TNF-α	Mm_Tnf_1_SG QuantiTect Primer Assay	QT00104006
IL-1β	Mm_Il1b_2_SG QuantiTect Primer Assay	QT01048355
COX-2	Mm_Ptgs2_1_SG QuantiTect Primer Assay	QT00165347
RPS18	Mm_Rps18_1_SG QuantiTect Primer Assay	QT00324940

2.7. Phagocytosis assay

RAW 264.7 cells were plated at a density of 45k cells/well in 96-well plate and exposed to CM derived from EGCs for 24 h, as described above. At the end of treatment, 0.0025% fluorescent yellow-green latex beads (Cat. No. #L1030; Merck) were added to each well for 90 min. CellMask™ Orange Plasma Membrane Stain (1:5000; Thermofisher) was added during the last 10 min of treatment for counterstaining. Cells were fixed using InsideFix Solution and mounted with DAPI-containing mounting solution (Merck). Digital images were captured with a Zeiss Observer.Z1 microscope from at least five random fields/condition. The total number of cells and the number of phagocytic cells were quantified by manual counting using the Analyze Particles plugin of the ImageJ software. Data were expressed as a percentage ratio between phagocytic cells and the total number of nuclei/field. To confirm internal bead localization, Z-stack digital images of selected single cells were captured using the Leica TCS-SP8 Confocal Laser Scanning Microscope at a 63X magnification and a 4x digital zoom and the 3D visualization module of the Leica Application Suite X (Las-X) software was used to generate the 3D volume rendering.

2.8. Transwell migration

RAW 264.7 cell migration was evaluated using a 24-well transwell chamber system with 8 μm pore membranes (Falcon). Macrophages (210 k/insert) were plated in the upper side of the transwell chamber, while EGCs (180k/well) were plated on the bottom of 24-well plates. Cells were co-cultured as described (see Cell Culture section). At the end of treatment, the non-migrating cells in the upper chamber of the transwell were removed with the aid of a cotton swab, while the cells migrated through the transwell membrane and adherent to its lower surface were fixed and stained using the Diff-Quik® (Dade Behring-Switzerland) kit, according to the manufacturer's instructions. Stained membranes were removed from the transwell plastic support with the aid of a scalpel and mounted on glass slides for microscopic analysis. Brightfield digital images from at least 3 random fields were captured at a 10X magnification. Analysis was carried out using the "Color deconvolution" plugin of the Fiji ImageJ software (Ruifrok and Johnston, 2001). Briefly, the image of the hematoxylin staining channel was converted to 8-bit before applying a threshold, and migrated cells were automatically counted with the aid of the Analyze Particles plugin.

2.9. Statistical analysis

All data were from at least three independent experiments run in replicates. All experimental values are presented as the mean ± SEM. Data were analyzed, by Student's t-test or one-way ANOVA followed by Uncorrected Fisher's LSD test for significance, as appropriate, using GraphPad Prism Software (GraphPad Software, San Diego, CA, USA). $p < 0.05$ was taken as the criterion for statistical significance.

3. Results

3.1. Establishment of the experimental model

The first part of the study focused on the establishment of the cellular model of enteroglial cells and their behavior in inflammatory conditions and in response to CsA, used as a tool to inhibit CN activity.

As depicted in Fig. 1 (top), we established an in-vitro model, where EGCs were exposed to the pro-inflammatory stimulus of LPS (5 μg/mL) for 24 h in combination with ATP (2 mM), added during the last hour of incubation. When CsA (1 μM) was used, it was always added 15 min before the inflammatory challenge. Samples were then processed for analysis of toxicity by MTT and protein expression by Western blot (WB) and immunocytochemistry (ICC). To study the interaction between enteric glia and immune system cells, we established an experimental model (Fig. 1, bottom) in which EGCs were activated with LPS + ATP for 5 h. Following removal of drugs, EGCs were either co-cultured with RAW 264.7 macrophages in a transwell migration assay carried out for 24 h or, alternatively, incubated for 18 h to collect CM. This was then transferred to RAW 264.7 macrophages for 6 h for qRT-PCR analysis or 24 h for phagocytosis assay.

Initially, a concentration-response curve of CsA was carried out using 0.5-20 μM CsA. High concentrations of CsA (starting at 5 μM) were found to cause reduction of EGCs growth, as shown by the MTT reduction assay (Fig. 2a). For this reason, a concentration of 1 μM was chosen for further experiments. The same assay was performed to establish the most appropriate inflammatory conditions to activate EGCs without causing cell death. While treatment for 24 h with LPS at the concentration of 5 μg/mL did not consistently induce an inflammatory response in EGCs (not shown), the addition of ATP 2 mM, applied during the last h of incubation, elicited significant changes (as shown in the following data) without causing any modification of cell viability (Fig. 2b). Treatment with LPS + ATP caused clear morphological changes of EGCs with reduction of branching and projections and a more flattened and round appearance, as shown in EGCs stained with the anti-TSG-6, a bioactive protein widely expressed in different cell types including astrocytes and involved in extracellular matrix interaction (Fig. 2c) (Coulson-Thomas et al., 2016; Ning et al., 2022; Srivastava et al., 2024).

3.2. Inflammatory induction in EGCs

The inflammatory profile of EGCs was assessed by examining the expression of GFAP, a marker of astrocytes expressed also in peripheral glial cells of the ENS. Data showed a slight but significant increase in GFAP protein levels when cells were treated with LPS + ATP (5 μg/mL-2 mM) for 24 h (Fig. 3a). CsA, added 15 min before the inflammatory insult, reverted this effect, while causing *per se* a reduction of GFAP expression in unstimulated EGCs (Fig. 3a). Similarly, treatment with LPS + ATP increased the expression of HMGB1 and the effect was sensitive to CsA pretreatment (Fig. 3a). To complete the inflammatory panel, the protein expression of the inflammasome component NLRP3 was analyzed by Western blot (Fig. 3b). Again, LPS + ATP (5 μg/mL-2 mM) slightly but significantly increased NLRP3 expression, and this effect was prevented under conditions of CN inhibition by CsA (1 μM) that, when added alone, was ineffective (Fig. 3b).

To analyze in more detail the effect of CsA on HMGB1 expression in inflammatory conditions, we tested whether there was a redistribution of HMGB1 within cellular compartments, by evaluating the percentage of $HMGB1^{+}$ nuclei by immunostaining (Fig. 3c–d). LPS + ATP (5 μg/mL-2 mM) were not able to modify the nuclear HMGB1 localization, but CsA (1 μM), only in the presence of inflammatory conditions, increased the amount of HMGB1+ nuclei. Finally, NF-κB p65 translocation in the cellular compartments was evaluated (Fig. 3e–f). As expected, nuclear localization of NF-κB p65 was increased by LPS + ATP exposure, as shown by immunostaining and such effect was blunted when CN was inhibited by CsA treatment. CsA alone did not show any effect compared to control (Fig. 3e–f).

3.3. Effects of activated enteric glial cells on immune cells

After characterizing the inflammatory profile of EGCs, the crosstalk between enteric glial cells and immune system cells was evaluated. To this end, we assessed a limited but representative set of markers and functional assays to evaluate macrophage activation.

Migration of RAW 264.7 macrophages towards pre-treated EGCs was evaluated using a transwell assay in a co-culture system, described in Fig. 1. The migration capacity of macrophages was quantified by automatically counting the number of hematoxylin-stained on the bottom side of the insert. Results obtained showed that pre-treatment of EGCs with LPS + ATP (5 μg/mL-2 mM) induced enhanced macrophage migration, by approximately 50% compared to control conditions

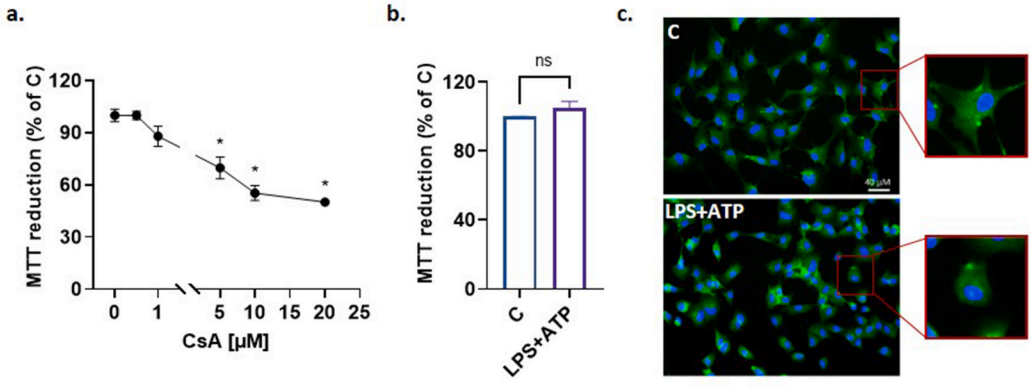

Fig. 2. Viability and morphological analysis of EGCs following treatments. The MTT reduction assay was carried out on cells exposed to cyclosporin A (CsA) in the concentration range of 0.5 to 20 μM for 24 h (a) and to an inflammatory stimulus consisting of LPS (5 μg/mL) for 24 h in combination with ATP (2 mM) during the last h (b). In c, immunostaining of TSG-6 (green) and nuclear counterstaining with DAPI (blue) under inflammatory conditions with LPS + ATP, compared to untreated control. Boxes report digital magnifications of representative cells for each condition. Bars are mean ± SEM of 5 (a) and 4 (b) independent experiments. *$p < 0.05$ vs C by one-way ANOVA followed by Fisher's-LSD (a).

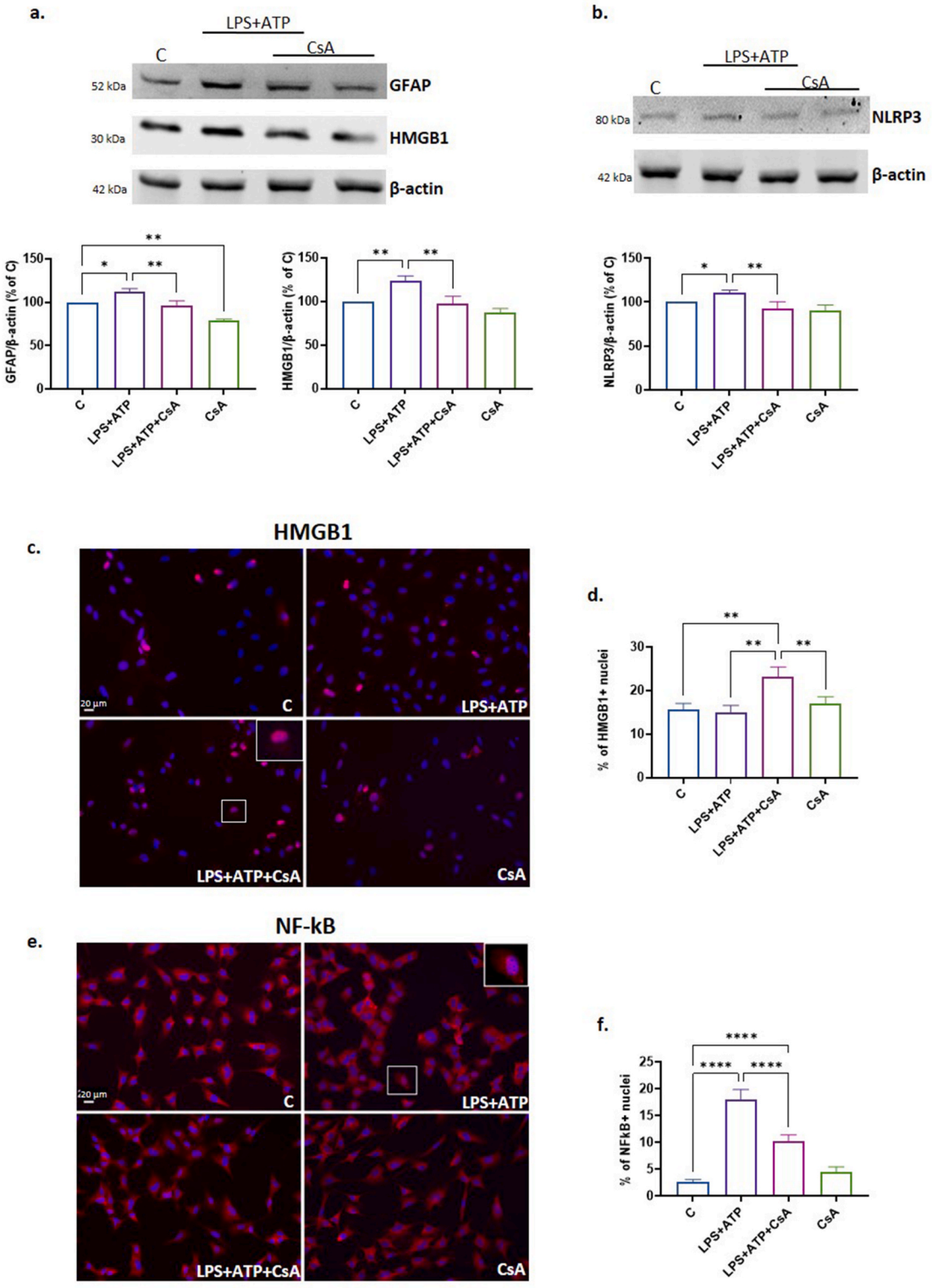

Fig. 3. Characterization of EGCs inflammatory profile. Cells were treated with LPS (5 μg/mL) + ATP (2 mM), LPS + ATP + CsA (1 μM), or CsA alone for 24h. Expression levels of GFAP and HMGB1 and of NLRP3 (b; n = 3) were assessed by Western blot and normalized over β-actin as a loading control and are expressed as percent vs the untreated control condition. Cells were immunostained for HMGB1 (red; c) and NF-κB p65 (red; e) and nuclear counterstaining was performed with DAPI (blue; c, e). The insets in c and e show nuclear positivity in representative cells at a higher magnification. The percentages of positive nuclei for each marker, over the total number of cells/field, is reported in d (n = 3) and f (n = 3). Bars are mean ± SEM of n independent experiments, as indicated. *$p < 0.05$, **$p < 0.01$, ***$p < 0.001$ and ****$p < 0.0001$ by one-way ANOVA followed by Fisher's-LSD post hoc test for significance. Scale bar = 20 μm. Representative blots (a, b) and immunostaining images (c, e) are reported.

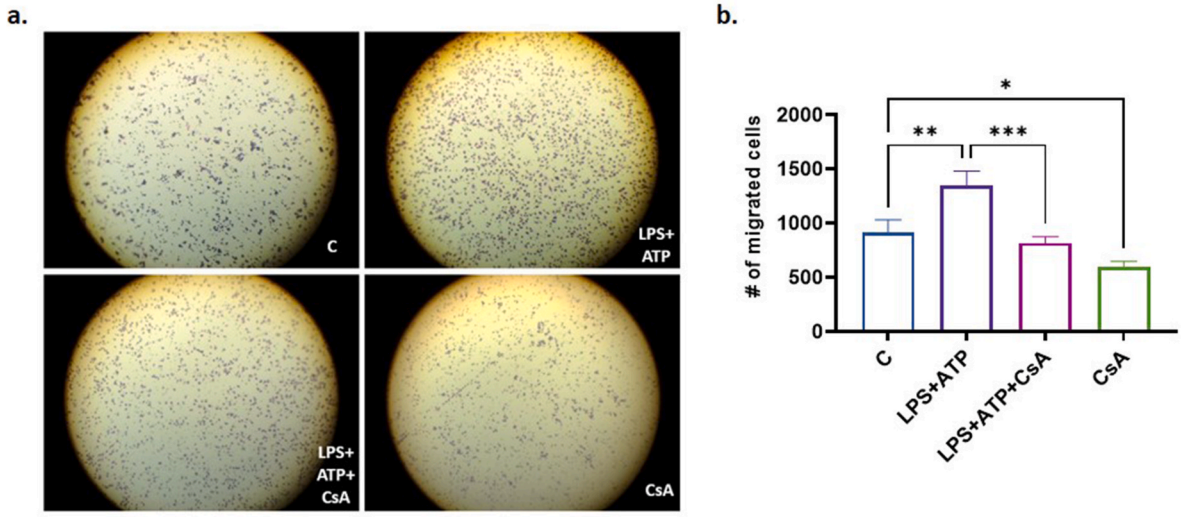

Fig. 4. Macrophage transwell migration assay. RAW 264.7 macrophages were cultured in transwell inserts in the presence of pre-treated EGCs for 24 h. Migrated macrophages, adhering to the bottom of the insert, were stained with hematoxylin (a) and their total number was graphed for each condition (b). Representative images of stained cells are reported in a. Bars are mean ± SEM of 3 independent experiments (b). *p < 0.05, **p < 0.01, ***p < 0.001 by one-way ANOVA followed by Fisher's-LSD post hoc test for significance.

(Fig. 4a and b). However, when in EGCs, CN activity was blocked by CsA (1 μM), the increased macrophage migration induced by the inflamed EGCs was prevented. A reduced migratory ability was observed in macrophages co-cultured with EGCs treated only with CsA (Fig. 4a and b).

The crosstalk between the two cell populations involved also the up-regulation, in macrophages, of pro-inflammatory genes chosen for their key role in M1-like activation. RAW 264.7 cells were treated for 6 h with CM collected from EGCs as described in Fig. 1 qRT-PCR analysis showed a marked increase of COX-2 (Fig. 5a) as well as of IL-1β and TNF-α (Fig. 5b and c). CsA, when added to LPS + ATP-treated EGCs, significantly reduced the inflammatory response observed in macrophages (Fig. 5a–c).

To further analyze the specific functional features of RAW 264.7 macrophages exposed to EGCs CM, phagocytic activity was examined after 24 h, using green fluorescent latex beads added during the last 90 min. Cells were counterstained with orange cell mask for the last 10 min of treatment and phagocytosed beads were detectable inside the cells (Fig. 6a and b). To validate the actual inclusion of beads, a laser confocal 3D analysis was carried out on selected cells (Fig. 6b). Results showed that the secretome from EGCs exposed to LPS + ATP did not affect phagocytic activity, while CN inhibition under these conditions led to a significant increase in phagocytosis. In contrast, treatment with CsA alone showed values comparable to control (Fig. 6c).

4. Discussion

IBD is an alarming global burden with an increasing incidence at a young age (Chen et al., 2025). Efficient therapeutical options are still lacking for a large number of patients, highlighting the need to identify new targets for intervention. In the scenario of enteric chronic inflammation, several actors are recognized to play a role, although immune cells have been best characterized. Accordingly, different classes of immunosuppressant drugs have proven beneficial and are largely used in therapy (Sokic-Milutinovic and Milosavljevic, 2024). In this context, enteric glial cells, which share many features with CNS astrocytes, have recently drawn attention as potential contributors to the onset and progression of IBD inflammation. Strikingly CN, the molecular target of

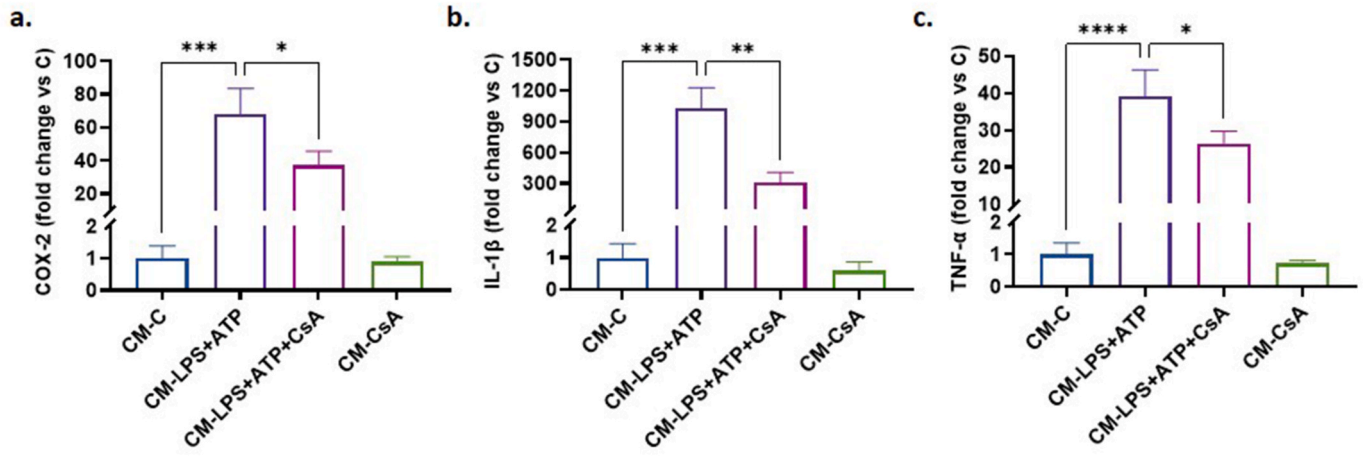

Fig. 5. mRNA expression of pro-inflammatory markers in macrophages. RAW 264.7 cells were exposed for 6 h to CM from EGCs pre-treated with LPS + ATP (5 μg/mL and 2 mM, respectively) alone or in the presence of CsA (1 μM), as indicated. qRT-PCR was carried out to analyze gene expression of COX-2 (a; n = 4), IL-1β (b; n = 4) and TNF-α (c; n = 6). Bars are mean ± SEM of n independent experiments, as indicated. *p < 0.05, **p < 0.01 and ***p < 0.001 by one-way ANOVA followed by Fisher's LSD test for significance.

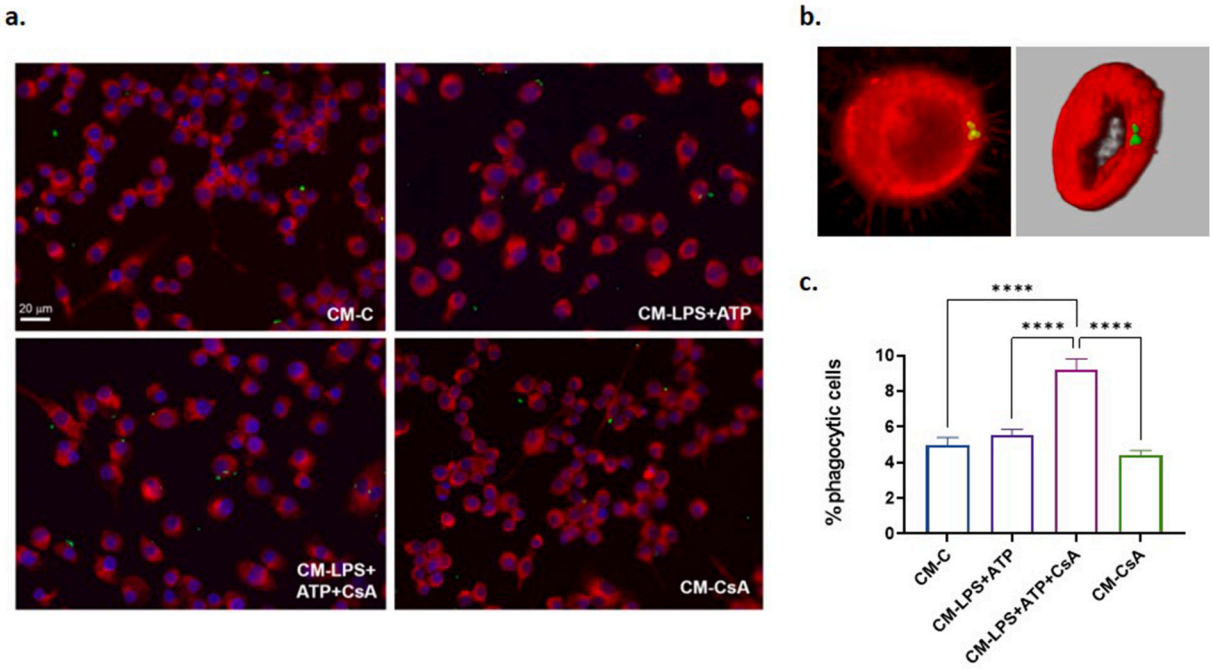

Fig. 6. Macrophage phagocytosis assay. RAW 264.7 cells were exposed for 24 h to CM from EGCs pre-treated as indicated. Fluorescent latex beads (green) and orange cell mask (red) were added during the last 90 min and 10 min of treatment, respectively. Nuclei were counterstained with DAPI (blue). In a, representative pictures are shown for each condition. In b, the confocal image of a representative cell that shows phagocytosed beads (left) with a 3D rendering (right). The number of cells with engulfed beads was counted and normalized to the total number of cells/field (c). Bars are mean ± SEM of 3 independent experiments. ****$p < 0.0001$ by one-way ANOVA followed by Fisher's LSD test for significance.

immunosuppressants such as CsA and tacrolimus, is a key mediator not only of T-cell activation, but also of astrocytic inflammation in the CNS. This led us to hypothesize that CN can similarly be involved in enteroglial responses to pro-inflammatory cues.

On these bases, the present study was carried out to investigate the involvement of CN in enteroglial pro-inflammatory activation and on the interplay with recruited immune cells, with the aim to refine our knowledge on the mechanism of action of CN-targeting immunosuppressants in IBD and potentially identify novel molecular targets.

To achieve our goal, we relied on an *in vitro* cross-talk model using EGCs and RAW 267.4 macrophages that, although with obvious limitations, allowed for an easier basic dissection of the cellular events and single contribution of each cell type to the effects under investigation. We initially characterized the inflammatory setting for enteroglial cells, exposing them to a combination of LPS and ATP. In our experience, astrocytic cells can easily acquire activated features when exposed to chemically defined conditions (Carbonaro et al., 2009) or to inflammatory stimuli. In this case, LPS and ATP were chosen since they have been shown to be increased in the altered intestinal wall in IBD *in vivo* models, providing a reliable *in vitro* setting (Ghosh et al., 2020; Jeong et al., 2025; Wan et al., 2016) that, however, cannot fully recapitulate chronic IBD-associated inflammation. Furthermore, we used CsA as a pharmacological tool to selectively inhibit CN. We confirmed the absence of toxicity to EGCs by both the inflammatory insult and the drug, and selected the concentration of 1 μM for CsA, which has been previously proven effective in glial cells *in vitro* (Gabryel et al., 2006). We then characterized the state of enteric gliosis induced by EGCs treatment with LPS + ATP. In particular, we investigated GFAP, a marker that is typically upregulated in activated astrocytes in the CNS under inflammatory conditions (Neunlist et al., 2014; Rosenbaum et al., 2016) and has been reported to be induced in subpopulations of enteric glia in both animal models and in humans (Grundmann et al., 2019). We further observed the induction of the NLRP3 component of the inflammasome, a key multiprotein complex acting as an effector of pathological inflammation (Coll and Schroder, 2025). This is in line with the acute inflammatory challenge applied, since ATP and LPS are known to synergistically activate NLRP3 also in macrophages (Pelegrin, 2021). ATP through the P2X7 receptor, has been suggested to directly engage the NLRP3 pathway. Although the mechanisms responsible for this interaction have not been fully elucidated, the decrease of intracellular K^+ and the massive increase of Ca^{2+} levels following activation of the P2X7 receptor are primarily invoked, envisaging a potential involvement of CN in these conditions (Ferrari et al., 1999). Accordingly, ATP has also been reported to activate NFAT by a CN-dependent pathway that required the influx of extracellular calcium (Ferrari et al., 1999), consistent with CN involvement following the ATP stimulus. Particularly interesting are the results related to total HMGB1 protein expression and its nuclear/cytosolic shuttling in activated EGCs. In the LPS + ATP condition, where total protein expression increases significantly, the nuclear localization is not modified. Conversely, while inhibition of CN prevents the increase in HMGB1 total expression caused by the inflammatory stimulus, it significantly increases its nuclear translocation. These results are in agreement with the literature reporting that nuclear HMGB1 plays a key role in homeostatic processes, including DNA repair, cell differentiation and during development (Guo et al., 2025). On the contrary, LPS has been shown to induce the acetylation of lysine residues, resulting in HMGB1 accumulating in the cytoplasm and preventing its return to the nucleus (Bonaldi et al., 2003). Notably, HMGB1 can even be released, acting as an alarmin. Extracellular HMGB1 can in fact significantly impact inflammation by activating alarm mechanisms through paracrine communication with neighboring immune cells (D'Antongiovanni et al., 2025; Guo et al., 2025). In our conditions, we observed an increase in HMGB1 total cell content during inflammation, not accompanied by nuclear upregulation. Although only a speculation, we could hypothesize a transient accumulation of the protein in the cytosol, which could precede its increased release. Further specific investigations, i.e. measurement of cytosolic and released HMGB1, could confirm such conjecture but were beyond the scope of this work. Such in-depth analyses surely warrant an intriguing new direction for future work. Given the central role of NF-κB p65 in inflammation and as a

downstream mediator of CN-driven signaling, we finally completed the profiling of EGCs inflammation by confirming the transcription factor's translocation into the nucleus. The ability of CsA to prevent or blunt all these responses validates the hypothesis that CN is directly involved in sustaining the inflammatory status in enteroglia challenged by external stimuli. Importantly, these data point to a parallel mechanism of action of the medication on both the immune system and on the ENS. From a pharmacological point of view, CsA is widely used as a CN inhibitor but it is important to note that, in astrocytes, it has been shown to exert also CN-independent effects, mainly by affecting mitochondrial function (Bambrick et al., 2006). Thus, while our data are fully consistent with CN inhibition, alternative or additional effects of CsA cannot be excluded.

Our observations on CN's pro-inflammatory role in EGCs are in agreement with its established action in the immune system, where it mediates activation of the NFAT/NF-κB p65 and IL-2 upregulation in T-cells (Furman and Norris, 2014). In addition, it is consistent with the well documented role of CN in pathological conditions in the CNS, where its dysfunctional activation contributes to sustain neuro-inflammation by activation of NFAT and NF-κB p65 signaling, as in T-cells (Sompol et al., 2017). However, many reports have shown that CN is also involved in homeostatic functions. Much interest has been focused in particular on the role of calcium-sensitive CN at the astrocytic level, being astrocytes homeostatic cells of the CNS that largely rely on Ca^{2+} signals (Verkhratsky et al., 2021). Recent studies have shown that the physiological roles of CN include maintaining basal protein synthesis and regulating neuronal functions such as excitability and memory formation (Lim et al., 2023). By analogy, it is not surprising that even in EGCs, CN is similarly endowed with a dual inflammatory/homeostatic action. In a recent study, knockout of CN in primary EGC cultures has been shown to alter their homeostatic functions and to increase expression of pro-inflammatory markers (Teramoto et al., 2023). Total CN ablation in these conditions likely leads to loss of the tightly regulated balance beween cell survival vs inflammatory functions of the phosphatase.

As mentioned above, a further aim of this work was to analyze the interaction of EGCs and recruited immune cells and more specifically to verify whether an EGC-directed anti-inflammatory action of CsA could also promote indirect effects on macrophages, the innate component of immune responses. In order to do this, we set up cross-talk conditions between EGCs and macrophages, where only the former were exposed to CsA. This model allowed us to demonstrate that the inflammatory state induced in EGCs promotes macrophage migration and their expression of a set of key pro-inflammatory genes such as COX-2, TNF-α and IL-1β. Furthermore, we showed that CsA can indirectly reduce such effects, completely or in part, by preventing EGCs inflammatory activation. Interestingly, our results also provide evidence that while the secretome of inflamed EGCs does not affect phagocytosis, the CM of EGCs challenged with LPS + ATP, under CN inhibition, promotes its increase. Literature regarding the actual interpretation of macrophage migration and phagocytosis in terms of M1-or M2-like type of activation appears so far conflicting. Migratory and phagocytic abilities are usually associated with M2-like macrophages, swiftly recruited to the sites of inflammation or injury, where they remove cellular debris and contribute to restoration of homeostasis (Atri et al., 2018; Yunna et al., 2020). However, there are also reports showing that LPS-stimulated M1 macrophages can display increased migration *in vitro* (Atri et al., 2018; Cui et al., 2019; Huang et al., 2023; Shapouri-Moghaddam et al., 2018; Zang et al., 2019). Moreover, it is well established that macrophages are highly dynamic cells that can rapidly change their phenotype along a continuum between two extremes, i.e. anti-inflammatory M2-like and pro-inflammatory M1-like. Consistently, more recent evidence has highlighted the existence of mixed phenotypes in pathological states, where M1-and M2-like features can overlap (Almansour et al., 2024; Cutolo et al., 2025; Das et al., 2015). In the enteric tract, previous work was carried out *in vivo* to study the pro-inflammatory cross-talk between activated EGC and resident macrophages of the external muscular layers (i.e. *muscularis* macrophages) during local inflammation. Results showed that EGCs were induced to proliferate and were activated to release the colony stimulating factor 1 (CSF1), in turn promoting macrophage differentiation into an anti-inflammatory/resolving phenotype (Stakenborg et al., 2022). In another study, *in vitro* and *in vivo* models were used to study the mechanisms of visceral pain. Here, EGCs were shown to promote macrophage activation via CSF1 by a connexin-43-dependent pathway, with an associated increase in macrophage migration and infiltration (Grubisic et al., 2020). It appears evident that, in general, responses are highly context-dependent, and different stimuli or time points of analysis and inflammatory levels may affect the final responses. In our model, results suggest that a sustained experimental pro-inflammatory state of enteric glia, by LPS + ATP, increases macrophage recruitment and sustains at least some of their pro-inflammatory features. In this context, CsA suppression of CN-mediated EGCs activation and in turn of macrophage activation, enhances their local phagocytosis. In an attempt to find an explanation for this apparent discrepancy, we can speculate that, under our experimental conditions, inflamed EGCs are able to activate the expression of key pro-inflammatory genes and recruit macrophages by enhancing their migration, likely indicative of an initial switch to M1-like features. When CN is inhibited and macrophages exhibit a blunted inflammatory response in regard to the genes we analyzed, their phagocytic capacity is activated, suggesting the transition to a reparative function, more likely associated with the M2-like phenotypic transition.

Our study addresses for the first time the effects of acute CN inhibition in the setting of inflammatory activation of enteric glial cells, taking into account the potential fallout on local macrophages. Our data offer a novel view of CN's role in enteric glia, beyond previous literature from models involving constitutive CN loss. From a translational point of view, our data seem to suggest that immunosuppression via CN-targeting drugs can inhibit recruitment of innate immune cells to distant sites by enteric glia, while enhancing their local homeostatic/inflammation-resolving functions.

CRediT authorship contribution statement

Aurora Patti: Writing – original draft, Methodology, Investigation, Formal analysis, Conceptualization. **Cristiana Lucia Rita Lipari:** Writing – review & editing, Investigation, Formal analysis, Conceptualization. **Armando Genazzani:** Writing – review & editing, Conceptualization. **Maria Angela Sortino:** Writing – review & editing, Writing – original draft, Supervision, Resources, Funding acquisition, Formal analysis, Conceptualization. **Sara Merlo:** Writing – review & editing, Writing – original draft, Supervision, Formal analysis, Data curation, Conceptualization.

Funding

This work was supported by PRIN2022 to MAS (grant #E53D23012080006) and by PIA.CE.RI from the University of Catania to SM and MAS (INTERACTIVE; grant #57722172152 and #20722142204).

Declaration of competing interest

The authors declare that they have no known competing financial interests or personal relationships that could have appeared to influence the work reported in this paper.

Acknowledgements

The authors wish to acknowledge the Bio-Nanotech Research And Innovation Tower (BRIT, University of Catania) for access to the confocal imaging facility.

References

Almansour, S., Dunster, J.L., Crofts, J.J., Nelson, M.R., 2024. Modelling the continuum of macrophage phenotypes and their role in inflammation. Math. Biosci. 377, 109289. https://doi.org/10.1016/j.mbs.2024.109289.

Atri, C., Guerfali, F.Z., Laouini, D., 2018. Role of human macrophage polarization in inflammation during infectious diseases. Int. J. Mol. Sci. 19. https://doi.org/10.3390/ijms19061801.

Bambrick, L.L., Chandrasekaran, K., Mehrabian, Z., Wright, C., Krueger, B.K., Fiskum, G., 2006. Cyclosporin A increases mitochondrial calcium uptake capacity in cortical astrocytes but not cerebellar granule neurons. J. Bioenerg. Biomembr. 38, 43–47. https://doi.org/10.1007/s10863-006-9004-7.

Bonaldi, T., Talamo, F., Scaffidi, P., Ferrera, D., Porto, A., Bachi, A., Rubartelli, A., Agresti, A., Bianchi, M.E., 2003. Monocytic cells hyperacetylate chromatin protein HMGB1 to redirect it towards secretion. EMBO J. 22, 5551–5560. https://doi.org/10.1093/emboj/cdg516.

Capoccia, E., Cirillo, C., Gigli, S., Pesce, M., D'Alessandro, A., Cuomo, R., Sarnelli, G., Steardo, L., Esposito, G., 2015. Enteric glia: a new player in inflammatory bowel diseases. Int. J. Immunopathol. Pharmacol. 28, 443–451. https://doi.org/10.1177/0394632015599707.

Carbonaro, V., Caraci, F., Giuffrida, M.L., Merlo, S., Canonico, P.L., Drago, F., Copani, A., Sortino, M.A., 2009. Enhanced expression of ERalpha in astrocytes modifies the response of cortical neurons to beta-amyloid toxicity. Neurobiol. Dis. 33, 415–421. https://doi.org/10.1016/j.nbd.2008.11.017.

Chen, L., Song, M., Yao, C., 2022. Calcineurin in development and disease. Genes Dis. 9, 915–927. https://doi.org/10.1016/j.gendis.2021.03.002.

Chen, L., Xu, Y., Ai, F., Shen, S., Luo, Y., Li, X., 2025. Dissecting the rising tide of inflammatory bowel disease among youth in a changing world: insights from GBD 2021. Int. J. Colorectal Dis. 40, 44. https://doi.org/10.1007/s00384-025-04821-0.

Cirillo, C., Sarnelli, G., Esposito, G., Grosso, M., Petruzzelli, R., Izzo, P., Cali, G., D'Armiento, F.P., Rocco, A., Nardone, G., Iuvone, T., Steardo, L., Cuomo, R., 2009. Increased mucosal nitric oxide production in ulcerative colitis is mediated in part by the enteroglial-derived S100B protein. Neuro Gastroenterol. Motil. 21. https://doi.org/10.1111/j.1365-2982.2009.01346.x, 1209-e1112.

Cirillo, C., Sarnelli, G., Esposito, G., Turco, F., Steardo, L., Cuomo, R., 2011. S100B protein in the gut: the evidence for enteroglial-sustained intestinal inflammation. World J. Gastroenterol. 17, 1261–1266. https://doi.org/10.3748/wjg.v17.i10.1261.

Coll, R.C., Schroder, K., 2025. Inflammasome components as new therapeutic targets in inflammatory disease. Nat. Rev. Immunol. 25, 22–41. https://doi.org/10.1038/s41577-024-01075-9.

Coulson-Thomas, V.J., Lauer, M.E., Soleman, S., Zhao, C., Hascall, V.C., Day, A.J., Fawcett, J.W., 2016. Tumor necrosis factor-stimulated Gene-6 (TSG-6) is constitutively expressed in adult central Nervous System (CNS) and associated with astrocyte-mediated glial scar formation following spinal cord injury. J. Biol. Chem. 291, 19939–19952. https://doi.org/10.1074/jbc.M115.710673.

Cui, S., Wu, Q., Wang, J., Li, M., Qian, J., Li, S., 2019. Quercetin inhibits LPS-induced macrophage migration by suppressing the iNOS/FAK/paxillin pathway and modulating the cytoskeleton. Cell Adhes. Migrat. 13, 1–12. https://doi.org/10.1080/19336918.2018.1486142.

Cutolo, M., Soldano, S., Smith, V., Gotelli, E., Hysa, E., 2025. Dynamic macrophage phenotypes in autoimmune and inflammatory rheumatic diseases. Nat. Rev. Rheumatol. 21, 546–565. https://doi.org/10.1038/s41584-025-01279-w.

D'Antongiovanni, V., Fornai, M., Colucci, R., Nericcio, A., Benvenuti, L., Di Salvo, C., Segnani, C., Pierucci, C., Ippolito, C., Nemeth, Z.H., Hasko, G., Bernardini, N., Antonioli, L., Pellegrini, C., 2025. Enteric glial NLRP3 inflammasome contributes to gut mucosal barrier alterations in a mouse model of diet-induced obesity. Acta Physiol. 241, e14232. https://doi.org/10.1111/apha.14232.

Das, A., Sinha, M., Datta, S., Abas, M., Chaffee, S., Sen, C.K., Roy, S., 2015. Monocyte and macrophage plasticity in tissue repair and regeneration. Am. J. Pathol. 185, 2596–2606. https://doi.org/10.1016/j.ajpath.2015.06.001.

Ferrari, D., Stroh, C., Schulze-Osthoff, K., 1999. P2X7/P2Z purinoreceptor-mediated activation of transcription factor NFAT in microglial cells. J. Biol. Chem. 274, 13205–13210. https://doi.org/10.1074/jbc.274.19.13205.

Fujita, M., Yagi, T., Okura, U., Tanaka, J., Hirashima, N., Tanaka, M., 2018. Calcineurin B1 deficiency in glial cells induces mucosal degeneration and inflammation in mouse small intestine. Biol. Pharm. Bull. 41, 786–796. https://doi.org/10.1248/bpb.b18-00041.

Furman, J.L., Norris, C.M., 2014. Calcineurin and glial signaling: neuroinflammation and beyond. J. Neuroinflammation 11, 158. https://doi.org/10.1186/s12974-014-0158-7.

Gabryel, B., Pudelko, A., Adamczyk, J., Fischer, I., Malecki, A., 2006. Calcineurin and Erk1/2-signaling pathways are involved in the antiapoptotic effect of cyclosporin A on astrocytes exposed to simulated ischemia in vitro. Naunyn-Schmiedebergs Arch Pharmacol 374, 127–139. https://doi.org/10.1007/s00210-006-0106-x.

Ghosh, S.S., Wang, J., Yannie, P.J., Ghosh, S., 2020. Intestinal barrier dysfunction, LPS translocation, and disease development. J Endocr Soc 4. https://doi.org/10.1210/jendso/bvz039.

Grubisic, V., McClain, J.L., Fried, D.E., Grants, I., Rajasekhar, P., Csizmadia, E., Ajijola, O.A., Watson, R.E., Poole, D.P., Robson, S.C., Christofi, F.L., Gulbransen, B. D., 2020. Enteric Glia modulate macrophage phenotype and visceral sensitivity following inflammation. Cell Rep. 32, 108100. https://doi.org/10.1016/j.celrep.2020.108100.

Grundmann, D., Loris, E., Maas-Omlor, S., Huang, W., Scheller, A., Kirchhoff, F., Schafer, K.H., 2019. Enteric glia: S100, GFAP, and beyond. Anat. Rec. 302, 1333–1344. https://doi.org/10.1002/ar.24128.

Guo, L., Wang, D., Jiang, X., He, G., 2025. HMGB1: from molecular functions to clinical applications in cancer and inflammatory diseases. Med. Res. Rev. https://doi.org/10.1002/med.70017.

Huang, S., Zheng, X., Dong, W., Lin, Y., Jiang, S., Zheng, H., Qian, C., 2023. Corydalis decumbens alleviates the migration, phagocytosis, and inflammatory response of macrophages. Evid. Based Complement. Alternat. Med., 7000477 https://doi.org/10.1155/2023/7000477, 2023.

Jeong, S., Park, S., Lee, D., Heo, G., Lee, Y., Rhee, S.H., Im, E., 2025. ATP mediates pyroptosis in the intestinal mucosal system during colitis. J. Cell. Physiol. 240, e70071. https://doi.org/10.1002/jcp.70071.

Kipanyula, M.J., Kimaro, W.H., Seke Etet, P.F., 2016. The emerging roles of the calcineurin-nuclear factor of activated T-Lymphocytes pathway in nervous system functions and diseases. J Aging Res, 5081021. https://doi.org/10.1155/2016/5081021, 2016.

Lim, D., Tapella, L., Dematteis, G., Talmon, M., Genazzani, A.A., 2023. Calcineurin signalling in astrocytes: from pathology to physiology and control of neuronal functions. Neurochem. Res. 48, 1077–1090. https://doi.org/10.1007/s11064-022-03744-4.

Liu, C., Yang, J., 2022. Enteric glial cells in immunological disorders of the gut. Front. Cell. Neurosci. 16, 895871. https://doi.org/10.3389/fncel.2022.895871.

Molkentin, J.D., 2004. Calcineurin-NFAT signaling regulates the cardiac hypertrophic response in coordination with the MAPKs. Cardiovasc. Res. 63, 467–475. https://doi.org/10.1016/j.cardiores.2004.01.021.

Neunlist, M., Rolli-Derkinderen, M., Latorre, R., Van Landeghem, L., Coron, E., Derkinderen, P., De Giorgio, R., 2014. Enteric glial cells: recent developments and future directions. Gastroenterology 147, 1230–1237. https://doi.org/10.1053/j.gastro.2014.09.040.

Ning, Y., Zhang, P., Zhang, F., Chen, S., Liu, Y., Chen, F., Wu, Y., Li, S., Wang, C., Gong, Y., Hu, M., Huang, R., Zhao, H., Guo, X., Wang, X., Yang, L., 2022. Abnormal expression of TSG-6 disturbs extracellular matrix homeostasis in chondrocytes from endemic osteoarthritis. Front. Genet. 13, 1064565. https://doi.org/10.3389/fgene.2022.1064565.

Ochoa-Cortes, F., Turco, F., Linan-Rico, A., Soghomonyan, S., Whitaker, E., Wehner, S., Cuomo, R., Christofi, F.L., 2016. Enteric glial cells: a new frontier in neurogastroenterology and clinical target for inflammatory bowel diseases. Inflamm. Bowel Dis. 22, 433–449. https://doi.org/10.1097/MIB.0000000000000667.

Okura, U., Hirashima, N., Tanaka, M., 2019. Calcineurin B1 deficiency in glial cells reduces gastrointestinal motility and results in maldigestion and/or malabsorption in mice. Biol. Pharm. Bull. 42, 1230–1235. https://doi.org/10.1248/bpb.b19-00124.

Pelegrin, P., 2021. P2X7 receptor and the NLRP3 inflammasome: partners in crime. Biochem. Pharmacol. 187, 114385. https://doi.org/10.1016/j.bcp.2020.114385.

Rosenbaum, C., Schick, M.A., Wollborn, J., Heider, A., Scholz, C.J., Cecil, A., Niesler, B., Hirrlinger, J., Walles, H., Metzger, M., 2016. Activation of myenteric glia during acute inflammation in vitro and in vivo. PLoS One 11, e0151335. https://doi.org/10.1371/journal.pone.0151335.

Ruifrok, A.C., Johnston, D.A., 2001. Quantification of histochemical staining by color deconvolution. Anal. Quant. Cytol. Histol. 23, 291–299.

Santhosh, S., Zanoletti, L., Stamp, L.A., Hao, M.M., Matteoli, G., 2024. From diversity to disease: unravelling the role of enteric glial cells. Front. Immunol. 15, 1408744. https://doi.org/10.3389/fimmu.2024.1408744.

Schneider, C.A., Rasband, W.S., Eliceiri, K.W., 2012. NIH image to ImageJ: 25 years of image analysis. Nat. Methods 9, 671–675. https://doi.org/10.1038/nmeth.2089.

Schneider, R., Schneider, L., Hamza, E., Leven, P., Wehner, S., 2025. The role of reactive enteric glia-macrophage interactions in acute and chronic inflammation. Neuro Gastroenterol. Motil. 37, e14947. https://doi.org/10.1111/nmo.14947.

Seguella, L., Gulbransen, B.D., 2021. Enteric glial biology, intercellular signalling and roles in gastrointestinal disease. Nat. Rev. Gastroenterol. Hepatol. 18, 571–587. https://doi.org/10.1038/s41575-021-00423-7.

Shapouri-Moghaddam, A., Mohammadian, S., Vazini, H., Taghadosi, M., Esmaeili, S.A., Mardani, F., Seifi, B., Mohammadi, A., Afshari, J.T., Sahebkar, A., 2018. Macrophage plasticity, polarization, and function in health and disease. J. Cell. Physiol. 233, 6425–6440. https://doi.org/10.1002/jcp.26429.

Sokic-Milutinovic, A., Milosavljevic, T., 2024. Inflammatory bowel disease: from conventional immunosuppression to biologic therapy. Dig. Dis. 42, 325–335. https://doi.org/10.1159/000535647.

Sompol, P., Furman, J.L., Pleiss, M.M., Kraner, S.D., Artiushin, I.A., Batten, S.R., Quintero, J.E., Simmerman, L.A., Beckett, T.L., Lovell, M.A., Murphy, M.P., Gerhardt, G.A., Norris, C.M., 2017. Calcineurin/NFAT signaling in activated astrocytes drives network hyperexcitability in abeta-bearing mice. J. Neurosci. 37, 6132–6148. https://doi.org/10.1523/JNEUROSCI.0877-17.2017.

Srivastava, T., Nguyen, H., Haden, G., Diba, P., Sowa, S., LaNguyen, N., Reed-Dustin, W., Zhu, W., Gong, X., Harris, E.N., Baltan, S., Back, S.A., 2024. TSG-6-Mediated extracellular matrix modifications regulate hypoxic-ischemic brain injury. J. Neurosci. 44. https://doi.org/10.1523/JNEUROSCI.2215-23.2024.

Stakenborg, M., Abdurahiman, S., De Simone, V., Goverse, G., Stakenborg, N., van Baarle, L., Wu, Q., Pirottin, D., Kim, J.S., Chappell-Maor, L., Pintelon, I., Thys, S., Pollenus, E., Boon, L., Van den Steen, P., Hao, M., Van Ginderachter, J.A., Boeckxstaens, G.E., Timmermans, J.P., Jung, S., Marichal, T., Ibiza, S., Matteoli, G., 2022. Enteric glial cells favor accumulation of anti-inflammatory macrophages during the resolution of muscularis inflammation. Mucosal Immunol. 15, 1296–1308. https://doi.org/10.1038/s41385-022-00563-2.

Suman, S., 2024. Enteric nervous system alterations in inflammatory bowel disease: perspectives and implications. Gastrointest Disord (Basel) 6, 368–379. https://doi.org/10.3390/gidisord6020025.

Tapella, L., Soda, T., Mapelli, L., Bortolotto, V., Bondi, H., Ruffinatti, F.A., Dematteis, G., Stevano, A., Dionisi, M., Ummarino, S., Di Ruscio, A., Distasi, C., Grilli, M.,

Genazzani, A.A., D'Angelo, E., Moccia, F., Lim, D., 2020. Deletion of calcineurin from GFAP-expressing astrocytes impairs excitability of cerebellar and hippocampal neurons through astroglial Na(+)/K(+) ATPase. Glia 68, 543–560. https://doi.org/10.1002/glia.23737.

Teramoto, H., Hirashima, N., Tanaka, M., 2023. Calcineurin B1 deficiency reduces proliferation, increases apoptosis, and alters secretion in enteric glial cells of mouse small intestine in culture. Cells 12. https://doi.org/10.3390/cells12141867.

Ulengin-Talkish, I., Cyert, M.S., 2023. A cellular atlas of calcineurin signaling. Biochim. Biophys. Acta Mol. Cell Res. 1870, 119366. https://doi.org/10.1016/j.bbamcr.2022.119366.

Verkhratsky, A., Parpura, V., Li, B., Scuderi, C., 2021. Astrocytes: the housekeepers and guardians of the CNS. Adv Neurobiol 26, 21–53. https://doi.org/10.1007/978-3-030-77375-5_2.

Wan, P., Liu, X., Xiong, Y., Ren, Y., Chen, J., Lu, N., Guo, Y., Bai, A., 2016. Extracellular ATP mediates inflammatory responses in colitis via P2 x 7 receptor signaling. Sci. Rep. 6, 19108. https://doi.org/10.1038/srep19108.

Yunna, C., Mengru, H., Lei, W., Weidong, C., 2020. Macrophage M1/M2 polarization. Eur. J. Pharmacol. 877, 173090. https://doi.org/10.1016/j.ejphar.2020.173090.

Zang, L., Wang, J., Ren, Y., Liu, W., Yu, Y., Zhao, S., Otkur, W., Zhao, Y., Hayashi, T., Tashiro, S.I., Onodera, S., Ikejima, T., 2019. Activated toll-like receptor 4 is involved in oridonin-induced phagocytosis via promotion of migration and autophagy-lysosome pathway in RAW264.7 macrophages. Int. Immunopharmacol. 66, 99–108. https://doi.org/10.1016/j.intimp.2018.11.014.

Zeng, Z., Mukherjee, A., Zhang, H., 2019. From genetics to epigenetics, roles of epigenetics in inflammatory bowel disease. Front. Genet. 10, 1017. https://doi.org/10.3389/fgene.2019.01017.